COBEM 2021 26th International Congress of Mechanical Engineering
November 22-26, 2021, Virtual Congress, Brazil

COB-2021-0477
INFLUENCE OF INCREMENTAL SHEET FORMING PARAMETERS ON FORM DEVIATION OF TITANIUM PARTS MEASURED BY COORDINATE MEASURING MACHINE AND 3D SCANNING THROUGH KINECT SENSOR

Felipe dos Anjos Rodrigues Campos
Leonardo Rosa Ribeiro da Silva
Federal University of Uberlândia-UFU, LEPU, 2121 João Naves de Ávila avenue, Uberlândia-MG, Brazil
filipin_anjos@hotmail.com ; leonardo.rrs@gmail.com

Felipe Chagas Rodrigues de Souza
Federal University of Uberlândia-UFU, LEPU, 2121 João Naves de Ávila avenue, Uberlândia-MG, Brazil
felipechagaslepu@gmail.com

Alisson Rocha Machado
Pontifice Catholic University-PUC-PR, 1155 Imaculada Conceição street, Curitiba-PR, Brazil
alissonr.machado@gmail.com

Abstract. *Significant technological advances in engineering have facilitated the production of parts for the medical industry, such as the Single Point Incremental Forming process (SPIF) for the conformation of customized parts in a reduced time. In this technique, the geometrical deviation of the surface and the system for its measurement are essential factors, given the difficulties of achieving close tolerances and obtaining accurate measurements quickly and cheaply. In this sense, the geometric conformity for medical applications of pure titanium cones formed by SPIF was evaluated in this work, in addition to comparing the measurement methodologies by 3D scanning with Kinect and by contact using a 3-coordinate measuring machine. From the comparison of shape deviations in relation to the theoretical cone and the surfaces measured by the two methods, the mean errors and mean standard deviations could be calculated, and 4D graphics showed the most deformed regions of the cones, which were the base and the top. The observed deviations were acceptable for many medical parts, while the use of Kinect proved to be feasible for fast, versatile, and highly economical verification of coarser tolerances on surfaces produced by SPIF.*

Keywords: *Single Point Incremental Forming, geometric deviation, titanium, 3D scanning, Kinect*

1. INTRODUCTION

In recent years, significant advances in engineering have enabled faster and cheaper production of implants and prostheses. Rapid prototyping methods based on CAD/CAM systems allowed the manufacture of custom patient parts from a 3D computer model at reduced lead time. Single Point Incremental Process is an example of such technology used to form thin metallic sheets without die and press. A sheet is fixed to the CNC machine table in this process, and a cylindrical tool moves against the plate to progressively deform it, as shown in Fig. 1. This makes the system easily adaptable to universal machining centers, very common in mechanical engineering laboratories and industry (Souza et al, 2020). Several materials and geometries can be produced at a lower cost than traditional methods regarding small batches and prototyping applications (Campos et al, 2020). For instance, this methodology has been successfully used to manufacture oral prostheses, bone implants for the face, shoulder, and knee (Cheng et al, 2020).

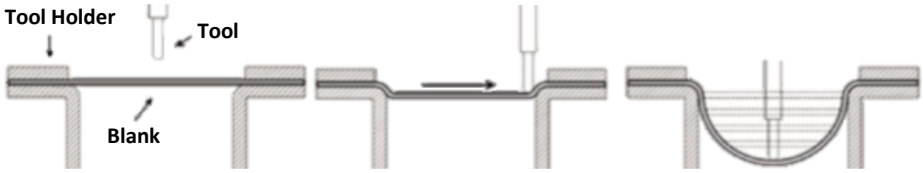

Figure 1. Representative scheme of the SPIF process. Adapted from Pereira et al (2018).

One of the main difficulties in this technique is geometric deviations due to the high deformations and stresses acting during forming. According to Hussain and Alkahtani (2021), the resulting ripples are intrinsic to the process and depend

on rotation speed, displacement, and tool diameter, besides the thickness and mechanical properties of the sheet material (Mateus et al, 2019; Oliveira et al, 2019). According to Wei et al, (2019), another problem is the elastic recovery after disengaging the tool, since the combination of stretching and bending of the sheet generates tensions within the elastic limit in some regions of the part. Thus, despite its flexibility in manufacturing biomedical items, verification and correction of shape deviations are complex challenges.

Geometric macro-imperfections can be evaluated by contact and non-contact measurement methods. The former is mainly represented by 3-coordinate measuring machines (MM3C), in which a measuring tip attached to a robotic or mechanical arm is moved over a part, recording the X, Y, and Z coordinates of the touched regions. The result is a point cloud used to reconstruct the object in 3D and calculate deviations from appropriate software. Although these devices have excellent resolution, on the order of micrometers, their operation is time-consuming, limiting the size of the sample (Ebrahim, 2015). Non-contact measurements, on the other hand, are generally much faster and able to extract thousands of points in a few milliseconds. These techniques are based on sensors that detect light or radiation reflected differently by the part under analysis, then using complex algorithms to distinguish the depth and contours of the object. Some of the techniques, popularly known as 3D scanning, have gained ground in metrological analysis and product inspection for the medical and manufacturing industries (Haleem and Javaid, 2019; Caruso et al, 2017). Other applications include planning cosmetic surgeries (Pöhlmann et al, 2017) and digitizing industrial environments (Nielsen et al, 2019).

In a previous work (Campos et al, 2021), the authors demonstrated the comparison between these measuring systems for pure titanium conical parts stamped by the SPIF process. In this work, similarly, the evaluation of the shape deviation was also carried out using two different methodologies for sampling the points: 3 coordinates measuring machine and 3D scanning with Kinect sensor, which is a commercial device based on the analysis of structured light by machine learning algorithms. However, besides assessing the accuracy of the second methodology for more SPIF parts, the influence of process parameters was also investigated. The measured points were used for 3D surface reconstruction using Matlab software, and a code in C++ language was developed to compare the accuracy and precision of formed parts. A design of experiments enabled the statistical analysis of the most important SPIF process parameters for form deviations.

2. METHODOLOGY

The single point incremental stamping tests were performed with 1 mm thick pure titanium plates, varying the tool rotation and feed speed, the vertical step, and the lubrication-coolant condition, as shown in Tab. 1. The formed material has good biocompatibility, but its low plasticity lowers its formability (Ambrogio et al, 2017). 5 mm radius semi-spherical point tools were used, turned from cylindrical steel bars of SAE 52100 steel. The tests were carried out in a ROMI Bridgeport 760 universal machining center with 9 kW maximum power, and cast-iron support was used for fixing the sheets. The equipment was adjusted to produce straight cones with a wall angle of 45° and a base diameter of 80 mm, with a height slightly less than 40 mm due to the tool radius. Figure 2(a) and Fig. 2(b) show, respectively, the theoretical cone and one of the produced cones, both vertically inverted in relation to the forming position.

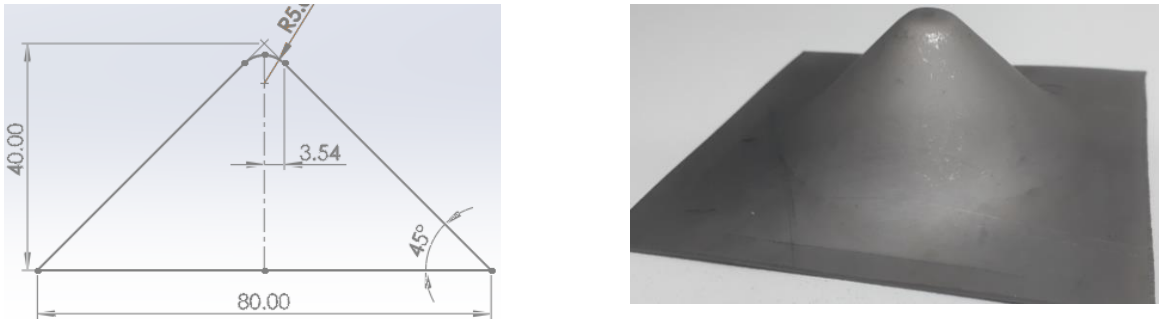

(a) (b)

Figure 2. (a) Dimensions of the theoretical cone (mm). (b) Example of part produced in SPIF tests.

Table 1. Process parameters of the SPIF tests.

Test	Rotation (rpm)	Feed speed (m/s)	Vertical step (mm)	Lubrication
1	75 (V-)	800 (f-)	0,8 (p+)	oil
2	150 (V+)	800 (f-)	0,5 (p-)	oil
3	75 (V-)	1200 (f+)	0,5 (p-)	oil
4	150 (V+)	1200 (f+)	0,8 (p+)	oil
5	10 (V-)	800 (f-)	0,5 (p-)	-
6	10 (V-)	1200 (f+)	0,5 (p-)	-
7	10 (V-)	800 (f-)	0,8 (p+)	-

Sampling of the outer surface of the cones was first made in a Mitutoyo 3-coordinate measuring machine, model BR-M443, mobile bridge type, manual, with a resolution of 1 µm. According to the calibration certificate and the work of Rosa (2016), when performing measurements with the part centered on the straightening table, the expanded uncertainty with 95% reliability in the three axes varies between 1.6 µm and 1.9 µm, with a palpation error of 1.9 ± 1.2 µm when using a 2 mm diameter ruby sphere. These values are much lower than the allowable errors with respect to theoretical parts typically manufactured by SPIF. Therefore, the reconstructed 3D surface measurements can be accepted as the actual dimensions of the part, from which the errors of the 3D scanning system will be calculated. 56 points were acquired in each cone, divided into 7 measuring planes along with its height, 3 on the straight part, 2 on the concave part of the top, and 2 on the convex part of the base, as shown in Fig. 3(a). In each plane, 8 approximately equidistant points were acquired, following the symmetry axes of the square base of the plate, as explained in Fig. 3(b). MM3C setup time is around 20 minutes, and each measurement requires approximately 10 minutes.

The Kinect sensor was fixed on a support with a horizontal and vertical distance of approximately 30 cm and 28 cm, respectively, aimed directly at the cones, placed in the center of a rotating table for surface sampling, as in the example of Fig. 3(c). This configuration is similar to that used by Zain and Raman (2020). Setup time is approximately 10 minutes, and each measurement requires around 3 minutes. This procedure ensured the same sampling conditions for each object, an essential factor since Corti et al (2016) and Gonzalez-Jorge et al (2013) showed that the metrological characteristics of systems based on Kinect could vary with the angle of incidence of the emitted radiation, with the position of the object in the captured frames, distance from the target to the sensor, and with the surface appearance and color of the studied object.

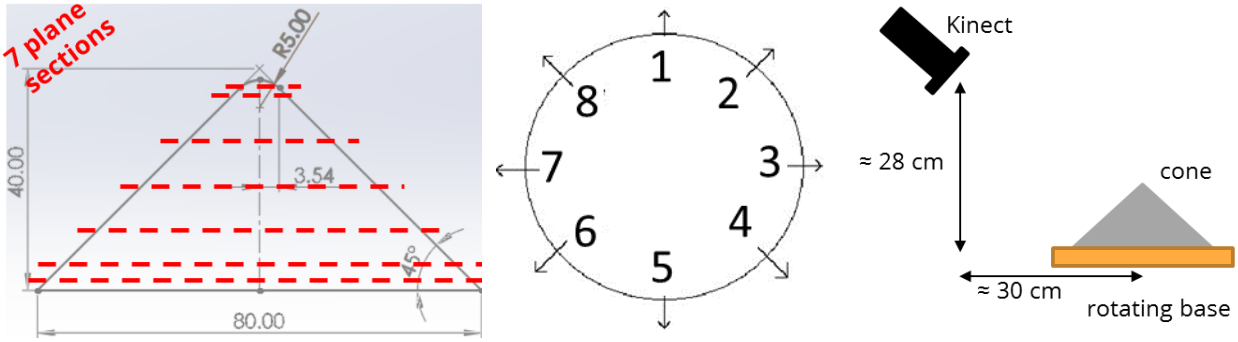

(a) (b) (c)

Figure 3. (a) Plane sections sampled at different heights of the cone in MM3C measurement. (b) Layout of the 8 point sampled for each plane section. (c) Arrangement of sensor and cone in Kinect measurements.

Skanect software version 1.10.2 was used to acquire the cloud with 500 points exported in STL format. In this type of file, a 3D shell of the object is formed from triangular elements joining the adjacent points, for which the Cartesian coordinates and the vectors representing the triangles that form the scanned surface are stored. Later, Blender software version 2.82 was used to center the points in relation to the origin of the coordinate system, as shown in Fig. 4(a), to facilitate comparison with the cone reconstructed from the MM3C. The new coordinates of the points were then exported into tables in TXT format, and can be seen in Fig. 4(b).

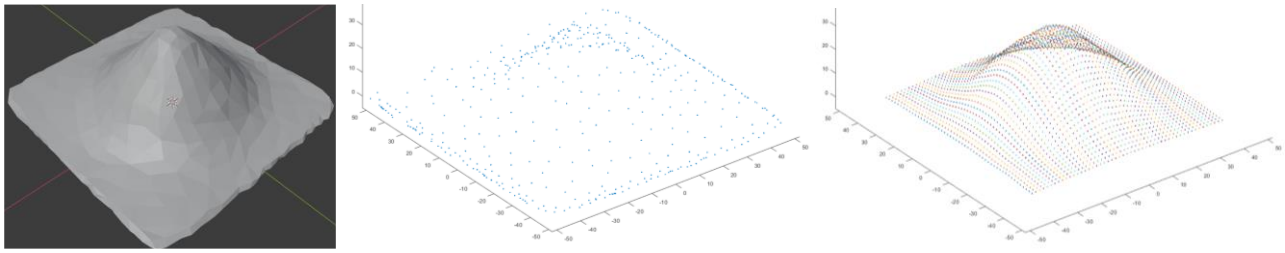

(a) (b) (c)

Figure 4. (a) STL cloud points scanned and opened in Blender. (b) Scanned cloud points plotted in Matlab from TXT data. (c) New cloud point recreated from *meshgrid* and *griddata* functions.

This data feed the algorithm developed in Matlab that reconstructs the surfaces through the *meshgrid* and *griddata* functions, which generate a new cloud of predetermined points in the XY plane with the Z coordinate interpolated from the original points, as displayed in Fig. 4(c). This strategy allows comparing equivalent points of clouds captured by the scanning system and by the MM3C. The reconstruction with these functions was made from a mesh of 2601 points (51 x 51) equally spaced in the XY plane, limiting -40 to 40 mm in each coordinate. Thus, under the methodology adopted by

Gonzalez-Jorge et al (2015), assuming the surface generated by the MM3C as a reference value, it is possible to calculate the mean error and mean standard deviation of the differences d_i for the total of N points associated with the measurement with Kinect, as in Eq. (1) and Eq. (2), respectively. Deviations from the theoretical cone were calculated by comparing the height of each point of the original cloud to the theoretical Z coordinate of the straight cone in Figure 2(a), for which the mean error and mean standard deviation can be calculated similarly. The theoretical value of Z can be expressed analytically according to Eq. (3), Eq. (4), and Eq. (5), deduced from the geometric relations of the cone, where the radius of the base (RB) is 40 mm, the radius tool radius (RF) is 5 mm, and the reference radius (Rref) is 3.54 mm, as indicated in Fig. 2(a).

$$e = \frac{1}{N}\sum_{i=1}^{N} d_i \tag{1}$$

$$s = \frac{1}{N-1}\sum_{i=1}^{N} (d_i)^2 \tag{2}$$

$$Base\ of\ sheet\ (Z = \ sheet\ thickness)\text{: } if\ \sqrt{X^2+Y^2} \geq RB, then\ Z = 1\ [mm] \tag{3}$$

$$Straight\ cone\text{: } if\ RB \geq \sqrt{X^2+Y^2} \geq Rref, then\ Z = RB - \sqrt{X^2+Y^2}\ [mm] \tag{4}$$

$$Round\ top\text{: } if\ \sqrt{X^2+Y^2} \geq Rref, then\ Z = RB - 2\cdot Rref + RF\cdot sen\left(\text{acos}\left(\frac{\sqrt{X^2+Y^2}}{RF}\right)\right)\ [mm] \tag{5}$$

3. RESULTS AND DISCUSSION

The reconstructions of cones by MM3C and 3D scan with the geometric deviation in relation to the theoretical cone for the conditions listed in Table 1 can be seen, respectively, in Fig. 5 and Fig. 6. The comparison between the 3D scan and the MM3C is similarly shown in Fig. 7. Both MM3C and 3D scan reconstructions of cones revealed recurrent patterns, such as higher base edges and lower top. The first factor is due to the bending of the edge due to the bending stress in this region since the process typically takes place under high forces in the Z direction, especially at the beginning of stamping. Although this type of imperfection correction requires variations that make the process more complex, such as using a forming die under the plate, the sheet base is cut out in many parts produced for the biomedical industry (Milutinović et al, 2021), remaining just the formed portion. The lower top corresponds to the final position of the tool in the process. In configurations such as this, the vertical force applied to the cone causes an unequal distribution of stresses in the vertical direction. This way, the elastic deformation of the rest of the cone reduces the stretching tension at the top's central point, reducing the plastic deformation necessary to deform the sheet and obtain the geometry.

According to metrological principles, the true measurand cannot be perfectly measured, as every measurement system contains uncertainty. Thus, the conventional or reference value must be obtained to verify the part's tolerances, using a measurement system with a resolution 10 times finer concerning the measurement system traditionally used (Vuolo, 1996). In this way, the conventional surface reconstructed from the point cloud probed in the MM3C can be compared to the surface generated by the 3D scanning. The predominantly green coloration is noticed, which indicates that the deviations compared point to point are close to 0 and are primarily contained in the range from -1 to 1 mm. These values are like those obtained by Bueno et al (2015) in evaluating the accuracy of different Kinect-type sensors. According to the authors, in the best configurations of part and sensor positioning during measurement, an accuracy between 0.5 and 1.0 mm can be obtained, which indicates the advantage of this measurement system for parts with larger tolerances, given the high versatility, practicality, and speed, in addition to the low cost of Kinect.

The mean from the theoretical cone based on Eq. (1) is quite close in the two measurement methods, as indicated by the green and orange bars in Fig. 8 for the evaluated conditions listed in Table 1. The high deviations in cones 3 and 5 are due to fractures that occurred during the process, relieving some of the stresses generated by the plastic deformation and lowering the dimensional accuracy of the final cone. The 3D scan maps show an area more sensitive to the deformations caused by the stress fields from the crack propagation. The blue bars in Fig. 8 indicate that the error between the 3D scan and the MM3C is generally smaller than the error between the measuring methods and the theoretical cone, indicating that both methods have a good agreement in the final measured values concerning the process deviations. The errors also oscillate between positive and negative, which indicates that they are from random nature instead of systematic. The mean standard deviation from the theoretical cone based on Eq. (2) is also quite close in the two measurement methods, as indicated by the green and orange bars in Fig. 9 for the evaluated conditions listed in Table 1. Again, the deviation between the measurement methods was lower than the difference between each method and the theoretical cone, reassuring that both methods are able to inspect these types of geometric deviations.

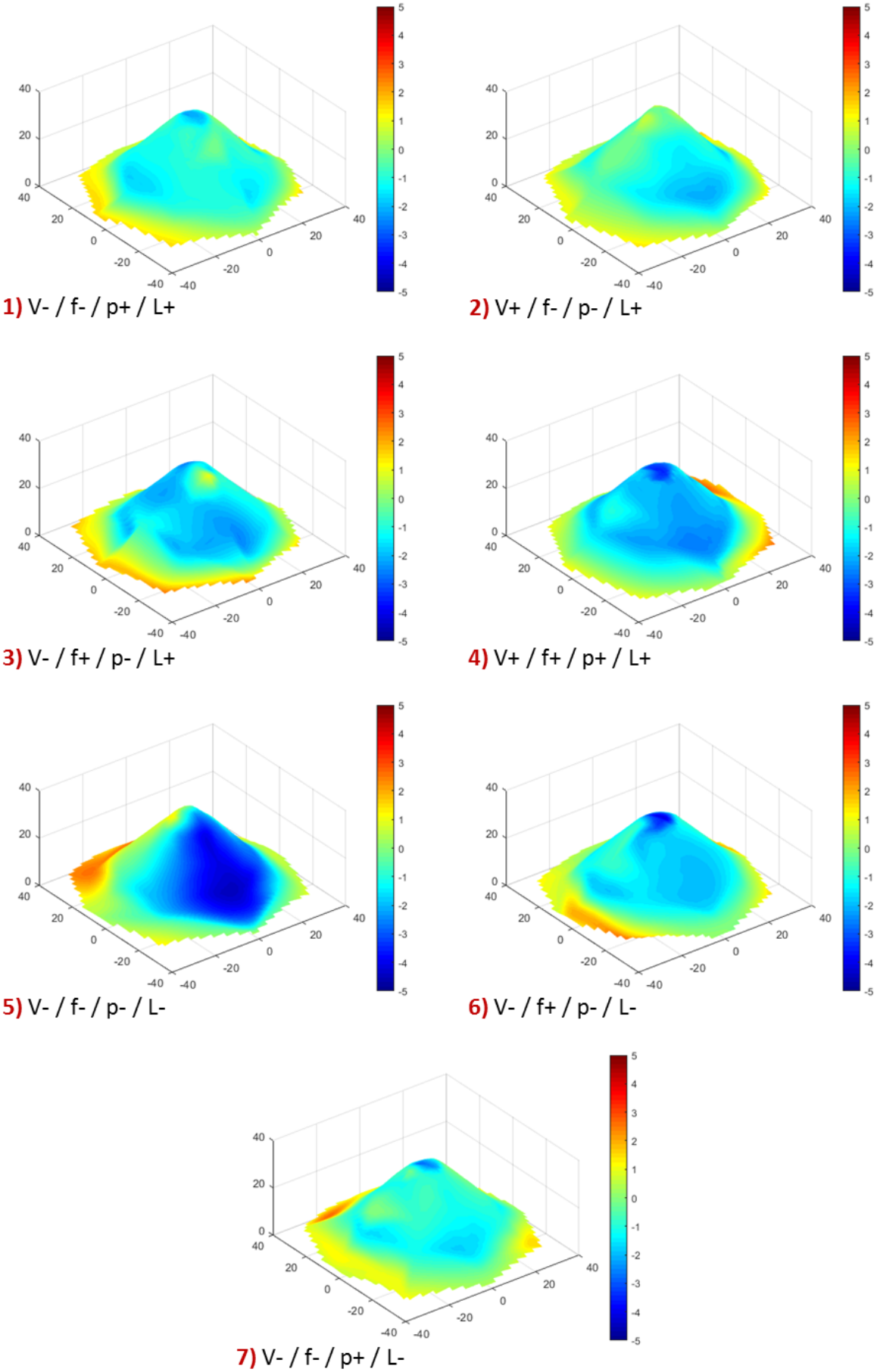

Figure 5. Geometric deviation of the cone measured by the MM3C in relation to the theoretical according to the parameters described in Table 1.

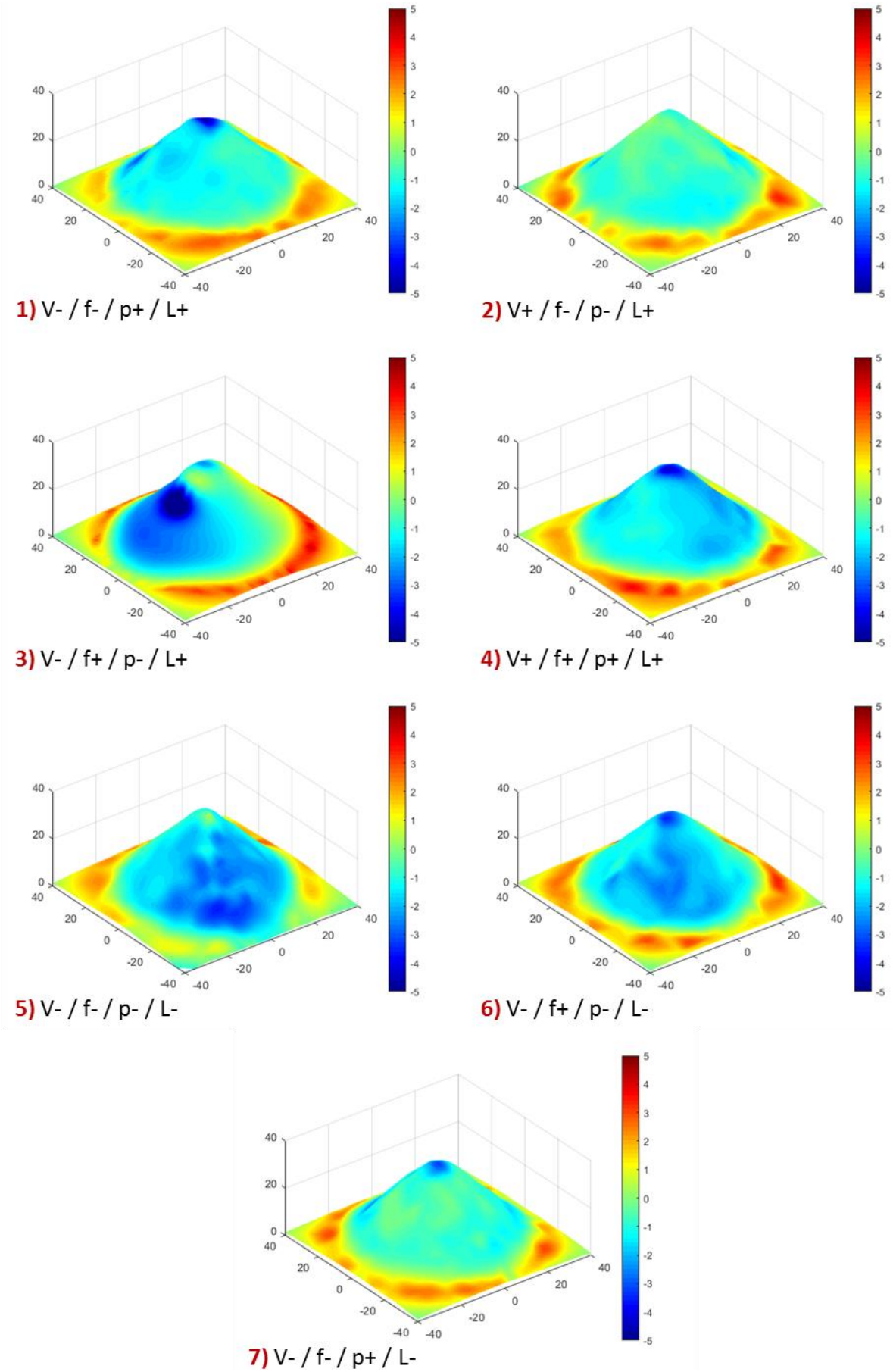

Figure 6. Geometric deviation of the cone measured by the 3D scan in relation to the theoretical according to the parameters described in Table 1.

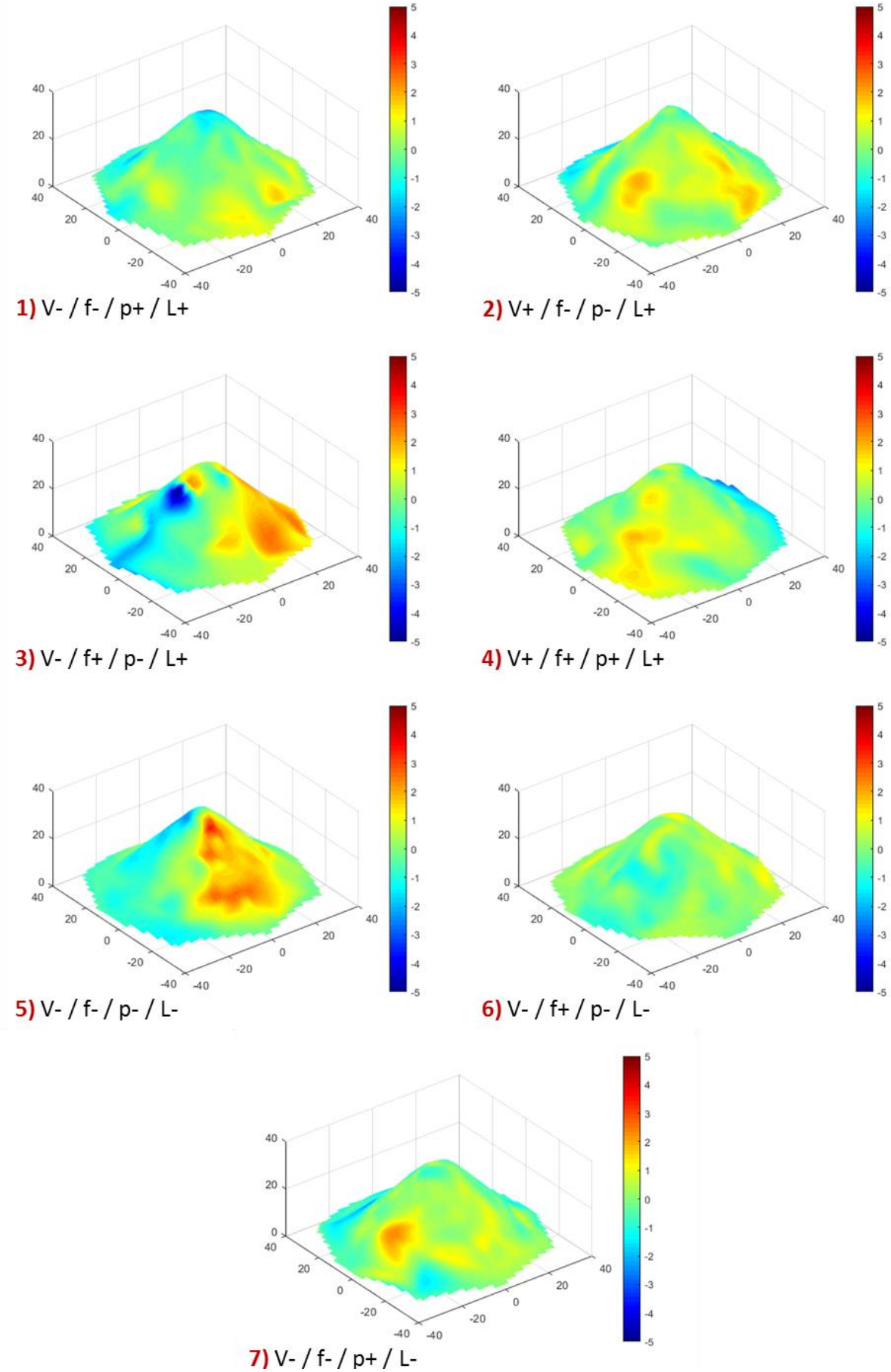

Figure 7. Geometric deviation of the cone measured by the 3DScan in relation to the MM3C according to the parameters described in Table 1.

Considering the precision of SPIF process, geometric deviations from the theoretical cone are also acceptable in many medical parts. For example, Milutinovic et al. (2021) produced stainless steel mouth prostheses with maximum deviations of around 0.815 mm, present at the edges of the piece. In this case, the application of resin in the borders was an inherent step in the process that would be sufficient to correct geometric distortions of up to 1.5 mm. In other studies (Cheng et al, 2020), more complex processes were used, such as double-point incremental forming (popularly known as two-point incremental forming or TPIF), to produce cranial implants in ultra-high molecular weight polyethylene (UHMWPE) with deviations of up to 0.5 mm. However, the edges showed 4 to 5 mm deviations. Thus, given the poor formability of titanium (Ambrogio et al, 2013) at lower temperatures, the values obtained for the average errors, smaller than 1.4 mm for the three cones, can be considered satisfactory.

Although the forming parameters have a decisive influence on the surface quality, residual stresses, and final shape of the stamped part, the differences observed for the cones were acceptable, with a mean standard deviation ranging from 0.995 to 1.700 mm. It is noteworthy that the maximum deviations in each cone were also evaluated, but they were not considered good metrics because they always occurred outside of the region of most interest. Furthermore, the complexity of comparing geometric deviations between surfaces through 3D scanning is highlighted. The method adopted in this work is based on the ISO 1101 (2017) standard, according to which the tolerance *t* for the deviation of any surface is given by the space delimited by two consecutive surfaces spaced at a distance of *t*. However, some authors adopt the comparison of specific points and geometric shapes, such as the center and radius of a sphere (Gonzalez-Jorge et al, 2013; Gonzalez-Jorge et al, 2015) or the height, diameter, and inclination of a cone (Rosa, 2016). Furthermore, some software only indicate the maximum deviation, calculated by the distance between two points from the coordinates (X, Y, Z).

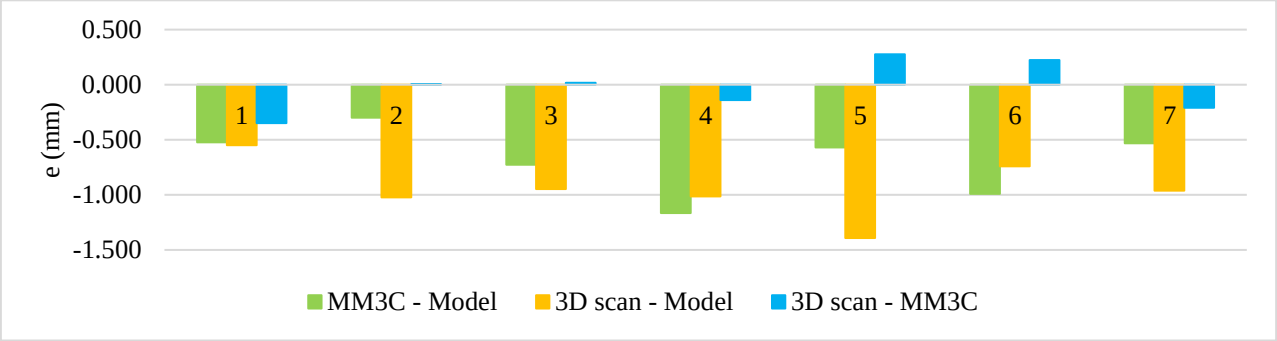

Figure 8. Average errors calculated by the deviations between the surfaces MM3C - theoretical, Scanned 3D - theoretical, Scanned 3D - MM3C.

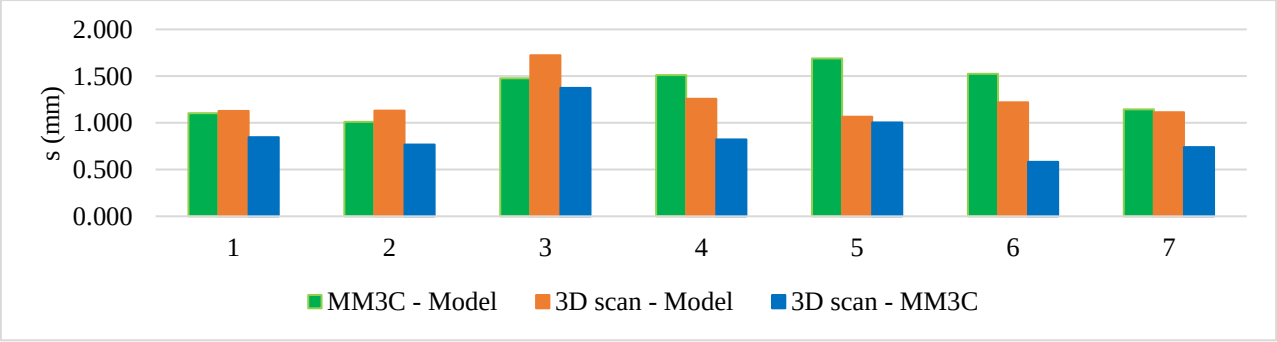

Figure 9. Mean standard deviations calculated by the deviations between the surfaces MM3C - theoretical, Scanned 3D - theoretical, Scanned 3D - MM3C.

Table 2. Student's t-test for the forming conditions evaluated.

p-values (two-sided)	MM3C - Model	
	e	s
V	0.8471	0.5593
f	0.0093	0.1018
p	0.6812	0.3434
L	0.9281	0.3505

Table 2 illustrates the Student's t-test, which is used to determine if the means of two sets of data are significantly different from each other. This test evaluated which process parameters influenced the cone error and deviation concerning the theoretical cone and the MM3C values since this measuring method is more reliable and presented relatively low deviation with the 3D scan. The p-values indicate that regarding the forming parameters, only the feed rate was significantly influential. The rotation and use of oil as lubricant were not influent because they affects more the surface roughness than the overall deformation rate of the blank. The vertical step also had low influence since SPIF is a rather lengthy process, giving the material time to relieve the stresses generated for the greater vertical steps in relation to the lower. Along with the vertical step, feed speed is the parameter that influences the overall mass dislocation during the forming process. However, differently from the vertical step, the feed speed dictates the rate and not only the direction of plastic deformation, explaining why this parameter had the most significant influence in the process.

4. CONCLUSIONS

The single-point incremental forming process was used to form cones from pure titanium sheets to assess geometric compliance for medical applications and compare measurement methodologies by 3D scanning with Kinect and contacting a measuring machine in 3 coordinates. From the comparison of shape deviations in relation to the theoretical cone and the surfaces measured by the two methods, the mean errors and mean standard deviations could be calculated, and 4D graphics showed the most deformed regions of the cones. From this information, the following conclusions can be listed:

• The tops of the cones were mostly between 0 and 3 mm and up to 5 mm lower than the planned part, due to this region being generated at the end of the process, when the sheet is under less stress and undergoes lower plastic deformation;

• The bases of the cones were bulging and their heights were up to 4 mm greater than for the theoretical cone due to the bending effect in this region, caused by the high vertical forces of the tool, especially at the beginning of the forming process;

• The mean errors and standard deviations of the surfaces generated by 3D scanning compared to the conventional contact method were low, in the ranges of -0.35 to +0.28 mm and 0.58 to 1.37 mm, respectively, indicating the feasibility of using Kinect as a tool to verify the geometric tolerances of some parts formed by SPIF;

• The geometric deviations of the formed parts are similar to those observed in other works in the manufacture of prostheses and implants, which attests to the effectiveness of this method as a tool to facilitate the customization of biomedical parts according to the patient specific needs at reduced lead time;

• The feed speed was the only significant parameter regarding the forming parameters, as it influences both forming direction and rate.

5. ACKNOWLEDGEMENTS

The authors are thankful to CNPq, FAPEMIG, and CAPES (Funding Code 01) for fostering postgraduate scholarships to the Metrology Teaching Laboratory and the Machining Teaching and Research Laboratory of the Federal University of Uberlândia for the support in carrying out the tests.

6. REFERENCES

Ambrogio, G., Gagliardi, F., Bruschi, S. e Filice, L., 2013. “On the high-speed Single Point Incremental Forming of titanium alloys”. *CIRP Annals*, Vol. 62, No. 1, p. 243-246.

Ambrogio, G., Sgambitterra, E., De Napoli, L., Gagliardi, F., Fragomeni, G., Piccininni, A., Gugleilmi, P., Palumbo, G., Sorgente, D., Barbera, L., Villa, T. M., 2017. “Performances analysis of titanium prostheses manufactured by superplastic forming and incremental forming”. *Procedia Engineering*, Vol. 183, p. 168-173.

Bueno, M., Díaz-Vilariño, L., Martínez-Sánchez, J., González-Jorge, H., Lorenzo, H. e Arias, P., 2015. “Metrological evaluation of KinectFusion and its comparison with Microsoft Kinect sensor”. *Measurement*, Vol. 73, p. 137-145.

Campos, F. A. R., Souza, F. C. R., Silva, L. R. R. and França, P. H. P., 2020. “Study of different lubri-coolant conditions for incremental sheet forming of thin zinc sheets”. *A Aplicação do Conhecimento Científico na Engenharia Mecânica*, Vol. 1, p. 21-34.

Campos, F. A. R., Silva, L. R. R., Paiva, L. F., Machado, A. R. and Assis, S. H. M., 2021. “Escaneamento 3D com Kinect comparado a máquina de medir por coordenadas na avaliação de desvio de forma em peças produzidas por estampagem incremental”. *In Proceedings of the XI Brazilian Congress of Manufacturing Engineering-COBEF2021, Curitiba-PR*.

Caruso, L., Russo, R. e Savino, S., 2017. "Microsoft Kinect V2 vision system in a manufacturing application". *Robotics and Computer-Integrated Manufacturing*, Vol. 48, p. 174-181.

Cheng, Z., Li, Y., Xu, C., Liu, Y., Ghafoor, S. e Li, F., 2020. "Incremental sheet forming towards biomedical implants: a review". *Journal of Materials Research and Technology*, Vol. 9, No. 4, p. 7225-7251.

Corti, A., Giancola, S., Mainetti, G. e Sala, R., 2016. "A metrological characterization of the Kinect V2 time-of-flight camera". *Robotics and Autonomous Systems*, Vol. 75, p. 584-594.

Ebrahim, M. A. B., 2015. "3D laser scanners' techniques overview". *International Journal of Science and Research*, Vol. 4, No. 10, p. 323-331.

Gonzalez-Jorge, H., Riveiro, B., Vazquez-Fernandez, E., Martínez-Sánchez, J. e Arias, P., 2013. "Metrological evaluation of Microsoft Kinect and Asus Xtion sensors". *Measurement*, Vol. 46, No. 6, p. 1800-1806.

Gonzalez-Jorge, H., Rodríguez-Gonzálvez, P., Martínez-Sánchez, J., González-Aguilera, D., Arias, P., Gesto, M. e Díaz-Vilariño, L., 2015. "Metrological comparison between Kinect I and Kinect II sensors". *Measurement*, Vol. 70, p. 21-26.

Haleem, A. e Javaid, M., 2019. "3D scanning applications in medical field: a literature-based review". *Clinical Epidemiology and Global Health*, Vol. 7, No. 2, p. 199-210.

Hussain, G. e Alkahtani, M., 2021. "Analysis of wall curling in incremental forming of a sheet metal: Role of residual stresses, stretching force and process conditions". *Journal of Materials Research and Technology*.

ISO 1101, 2017. "Geometrical product specifications (GPS) - geometrical tolerancing - tolerances of form, orientation, location and run-out". *International Organization for Standardization*.

Mateus, V. V. G., Silva, L. R. R., Campos, F. A. R., França, P. H. P., Barreto, J. C. N. e Sales, W. F., 2019. "Efeito da rotação na estampagem incremental de chapas de aço AISI 304". *Revista Sciencomm*, Vol. 8, p. 37-43.

Milutinović, M., Lendjel, R., Baloš, S., Zlatanović, D. L., Sevšek, L. e Pepelnjak, T., 2021. "Characterisation of geometrical and physical properties of a stainless steel denture framework manufactured by single-point incremental forming". *Journal of Materials Research and Technology*, Vol. 10, p. 605-623.

Nielsen, C. P., Malik, A. A., Hansen, D. G. e Bilberg, A., 2019. "Low-Cost 3D Scanning in a Smart Learning Factory". *Procedia Manufacturing*, Vol. 38, p. 824-831.

Oliveira, B. J., Silva, L. R. R., Campos, F. A. R., França, P. H. P., Mateus, V. V. G., Barreto, J. C. N. e Sales, W. F., 2019. "Análise da velocidade de avanço na estampagem incremental do aço AISI 304". *Revista Sciencomm*, Vol. 8, p. 14-22.

Pereira, L. C., de Paula Santos, G. H., da Silva, M. L. N. e Goulart, P. R., 2018. "Determinação da estampabilidade do latão 70/30 pelo processo de Estampagem Incremental de Ponto Simples". *Anais do X Congresso Brasileiro de Engenharia Mecânica - CONEM-2018*, Salvador, BA.

Pöhlmann, S. T., Harkness, E., Taylor, C. J., Gandhi, A. e Astley, S. M., 2017. "Preoperative implant selection for unilateral breast reconstruction using 3D imaging with the Microsoft Kinect sensor". *Journal of Plastic, Reconstructive & Aesthetic Surgery*, Vol. 70, No. 8, p. 1059-1067.

Rosa, V. A. D. O., 2016. *Avaliação do desempenho metrológico dos métodos de ajuste utilizados nas máquinas de medir por coordenadas*. Tese de doutorado, Universidade Federal de Uberlândia, Uberlândia.

Souza, F. C. R., Silva, L. R. R., Campos, F. A. R. e Peixoto, A. C. S., 2020. "Manufacture of complex parts in thin sheets of commercially pure aluminum using incremental sheet forming method". *A Aplicação do Conhecimento Científico na Engenharia Mecânica*, Vol. 1, p. 11-20.

Vuolo, J. H., 1996. *Fundamentos da teoria de erros*. Editora Blucher, São Paulo, 2ª ed.

Wei, H., Zhou, L., Heidarshenas, B., Ashraf, I. K. e Han, C., 2019. "Investigation on the influence of springback on precision of symmetric-cone-like parts in sheet metal incremental forming process". *International Journal of Lightweight Materials and Manufacture*, Vol. 2, No. 2, p. 140-145.

Zain, N. E. and Rahman, W. N., 2020. "Three-dimensional (3D) scanning using Microsoft® Kinect® Xbox 360® scanner for fabrication of 3D printed radiotherapy head phantom". *Journal of Physics: Conference Series*, Vol. 1497, No. 1, p. 012005.

7. RESPONSIBILITY NOTICE

The authors are the only responsible for the printed material included in this paper.